

**LECTURE NOTES**

**1- Seismic waves**

**1.1- General elastic wave equation**

Consider the application of forces to an infinitesimal cube in an elastic medium (Fig 1):

$$mass \times acceleration = \sum forces \tag{1}$$

$$\rho \frac{\partial^2 u_i}{\partial t^2} = \sigma_{ij,j} + f_i \tag{2}$$

$$\rho \frac{\partial^2 u_i}{\partial t^2} = c_{ijkl} u_{(k,l),j} + f_i \tag{3}$$

where

- $\rho$ : density
- $u_i$ : displacement
- $t$ : time
- $\sigma_{ij}$ : stress tensor
- $f_i$ : body forces
- $c_{ijkl}$ : elastic tensor
- $i,j,k,l$ : x|y|z

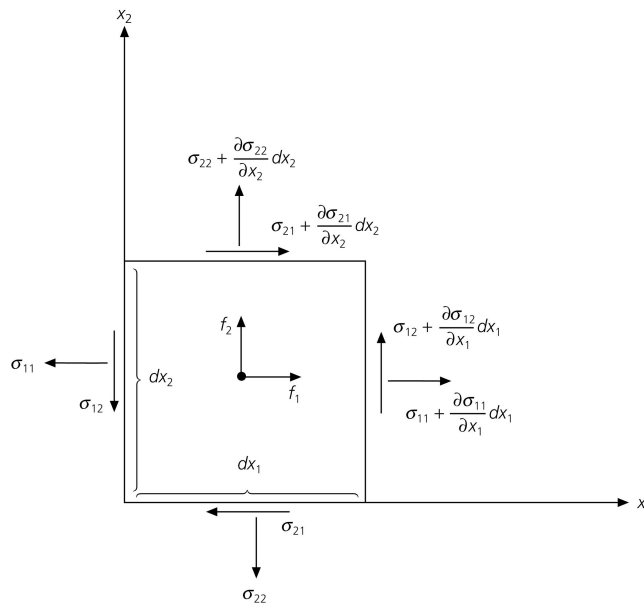


Fig 1. Forces applied to infinitesimal cube (Stein and Wysession, 2003)

## 1.2- Seismic wave equation for a homogeneous, isotropic medium (P-waves, S-waves)

For an isotropic medium, the elastic tensor depends only on two parameters, the Lamé parameters  $\lambda$  and  $\mu$ , such that  $c_{ijkl} = \lambda\delta_{ij}\delta_{kl} + \mu(\delta_{il}\delta_{jk} + \delta_{ik}\delta_{jl})$ , and the elastic wave equation can be decomposed into two equations (see Fig 2).

We use Helmholtz decomposition to partition the displacement into two potentials:

$$\underline{u} = \underline{\nabla}\phi + \underline{\nabla} \times \underline{\psi} \quad (4)$$

where,

$\phi$  is a scalar potential that is rotation free ( $\underline{\nabla} \times \underline{\nabla}\phi = 0$ ),

$\underline{\psi}$  is a vector potential that is divergence free ( $\underline{\nabla} \cdot \underline{\nabla} \times \underline{\psi} = 0$ ).

Substituting into (3) and collecting terms yields two independent equations for

P-waves:

$$\alpha^2 \underline{\nabla}^2 \phi - \frac{\partial^2 \phi}{\partial t^2} = -\frac{1}{\rho} F_P \quad (5)$$

with velocity

$$\alpha = \sqrt{\frac{\lambda + 2\mu}{\rho}} \quad (6)$$

S-Waves:

$$\beta^2 \underline{\nabla}^2 \underline{\psi} - \frac{\partial^2 \underline{\psi}}{\partial t^2} = -\frac{1}{\rho} F_S \quad (7)$$

with velocity

$$\beta = \sqrt{\frac{\mu}{\rho}} \quad (8)$$

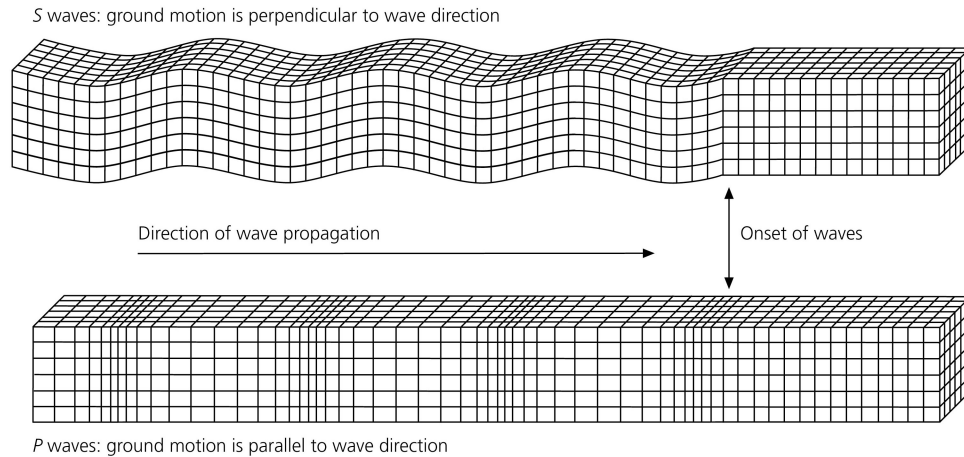


Fig 2. P- and S- waves (Stein and Wysession, 2003)

### 1.3- Ray theory

Infinite frequency approximation: seismic energy that travels between a source and receiver in a uniform, isotropic space is confined to discrete rays, as in ray optics (see Fig 3).

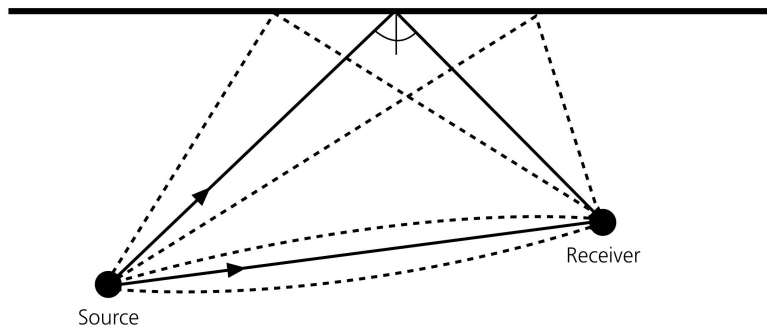


Fig 3. Seismic rays (Stein and Wysession, 2003)

### 1.4- Snell's Law

When a seismic ray travels across a welded interface between two media (Fig 4), there is continuity of displacement and traction at the boundary.

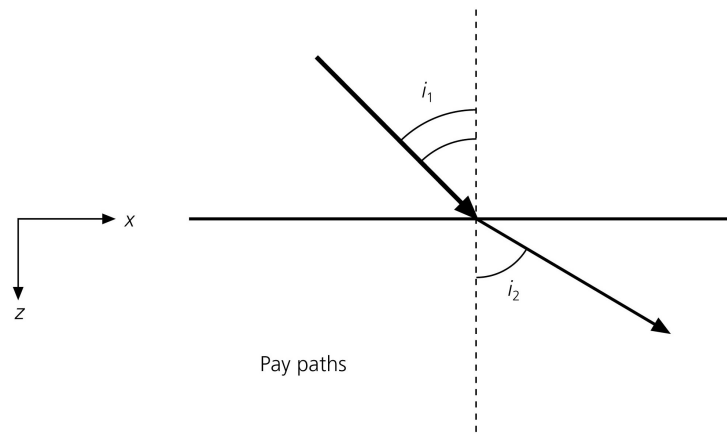


Fig 4. Ray transmission across a welded interface between two media (Stein and Wysession, 2003).

The angles of incidence and reflection/transmission of the ray (angles between the ray and the normal to the interface) depend on the velocity in each medium, and are related through Snell's law:

$$p = \frac{\sin i_1}{v_1} = \frac{\sin i_2}{v_2} \quad (9)$$

where  $p$  is the ray parameter (a constant quantity for given rays across a horizontally-layered model),  $i_n$  is the incidence/transmission angle of the ray in medium  $n$ , and  $v_n$  is

the velocity in medium  $n$ . Due to boundary conditions at the interface, the energy of an incident P- or SV-wave undergoes transmission, reflection, and partial conversion (Fig 5).

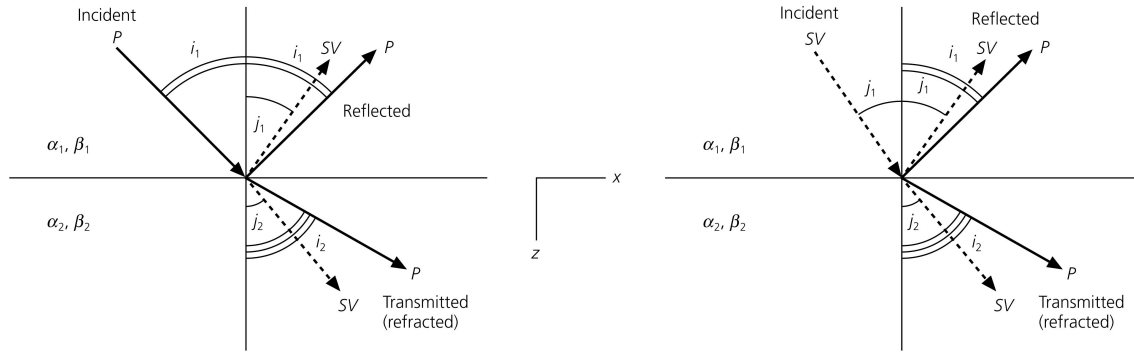


Fig 5. Transmitted and reflected waves for incident P and SV waves (Stein and Wysession, 2003)

For a given ray parameter  $p$ , the angle of incidence increases with increasing velocity, which means that the ray approaches the plane of the interface with increasing velocity. This is a desirable attribute for smooth regional subsurface models of the earth, which exhibit a general increase in seismic velocity with depth, as it insures that waves generated at a source near the surface travel back to the surface! This also means that for a critical incidence angle  $i_c$ , the wave transmitted from a low-velocity to a high-velocity medium will travel parallel to the interface, through the high-velocity medium (Fig 6). This wave is called a *refracted wave*, or also a *head wave*. Beyond the critical angle, there is no transmission into the high-velocity medium.

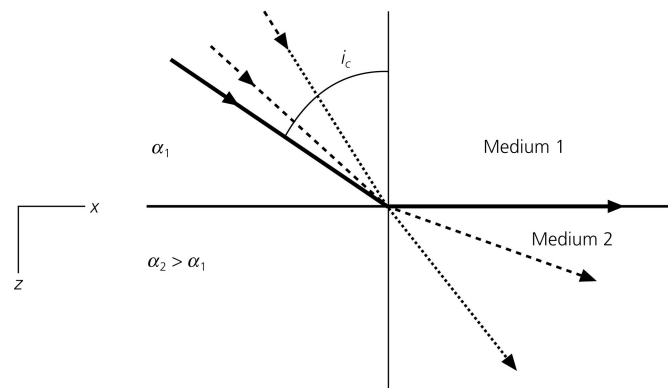


Fig 6. Critical angle for P-waves incident upon a boundary. Transmitted S and reflected P and S waves should also be present but they are not shown (Stein and Wysession, 2003).

Seismic reflection and refraction techniques rely on the interactions between seismic waves at welded interfaces to determine the spatial distribution of these interfaces and the seismic velocities of the media they separate (Fig 7). In the next sections, we provide a brief overview of these techniques for applications to simple layered earth models.

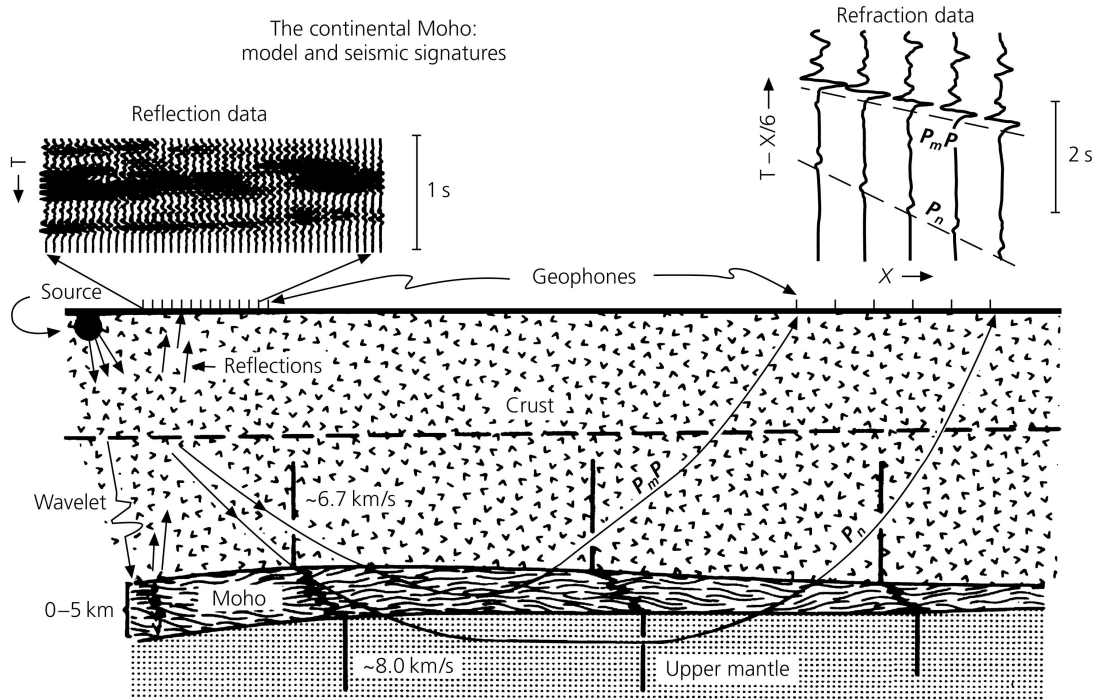


Fig 7. Seismic reflection and refraction experiments at crustal scale (Stein and Wysession, 2003)

## 2- Seismic refraction

In applications to horizontally layered earth models, the refraction technique is used to estimate the thickness and velocity of the layers. It relies on the identification of P- or S-arrivals, especially those of refracted (head) waves, at long offsets ( $\sim 0-5$  times the depth of investigation). P-waves are more practical because they are the first to arrive at the receivers and because they produce mostly vertical ground motion that can be measured by single component geophones.

### 2.1- Layer over a half-space

First, we consider a simple model consisting of a layer over a half-space (Fig 8). A receiver located at a distance  $x$  from the source ( $x=0$ ) will record up to three P-wave arrivals depending on the offset: a direct wave, a reflected wave, and a head wave. These arrivals can be picked directly on sections that display seismograms as a function of offset (Fig 9-10).

Travel times as a function of distance from the source are given by the following expressions:

$$T_D(x) = \frac{x}{v_0} \quad (10)$$

$$T_R(x) = 2 \frac{\left(\frac{x^2}{4} + h_0^2\right)^{1/2}}{v_0} \quad (11)$$

$$= px + 2\eta_0 h_0$$

$$T_H(x) = \frac{x}{v_1} + 2h_0 \left(\frac{1}{v_0^2} - \frac{1}{v_1^2}\right)^{1/2} \quad (12)$$

$$= \frac{x}{v_1} + \tau_1$$

where

$T_D, T_R, T_H$ : travel times of the direct, reflected and head wave, respectively

$x$ : distance between the source and the receiver (offset)

$v_n$ : seismic velocity in medium  $n$

$\eta_0$ : vertical component of slowness in the upper layer,  $\eta_0 = \left(1/v_0^2 - p^2\right)^{1/2}$

$h_0$ : thickness of the upper layer (layer 0)

$\tau_1$ : time axis intercept of the head wave refracted in the half space (layer 1).

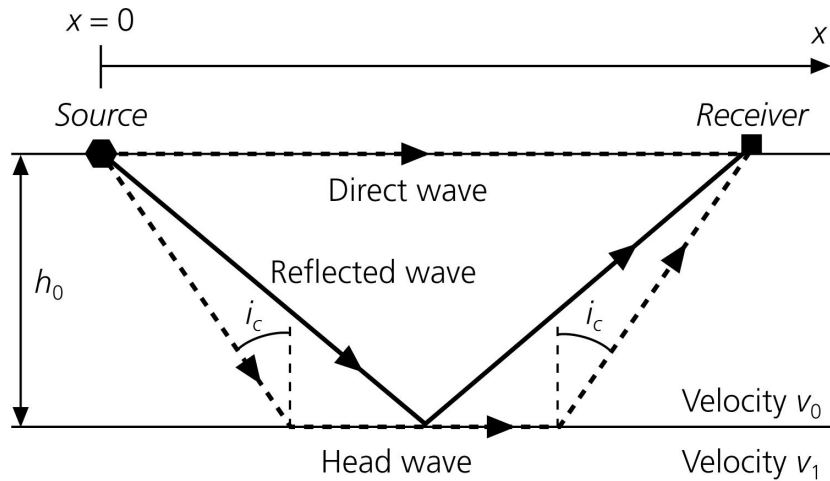


Fig 8. Ray paths for a layer over a half-space (Stein and Wysession, 2003)

Therefore, to characterize a model consisting of a layer over a half-space in seismic refraction, follow these steps:

- 1) plot the seismograms as a function of offset (Fig 9a);
- 2) pick the arrival times of the various phases and connect the picks to obtain travel time curves (Fig 9b);
- 3) estimate  $v_0$  and  $v_1$  from the slopes of the travel time curves (Fig 9b);
- 4) obtain  $\tau_1$  from the intercept of the head wave's travel time curve and the time axis (Fig 9b);
- 5) estimate the thickness of the upper layer,  $h_0$ , by using estimates of  $v_0, v_1$  and  $\tau_1$  in eq. 12 for  $x=0$  km and  $T_H(x) = \tau_1$ .

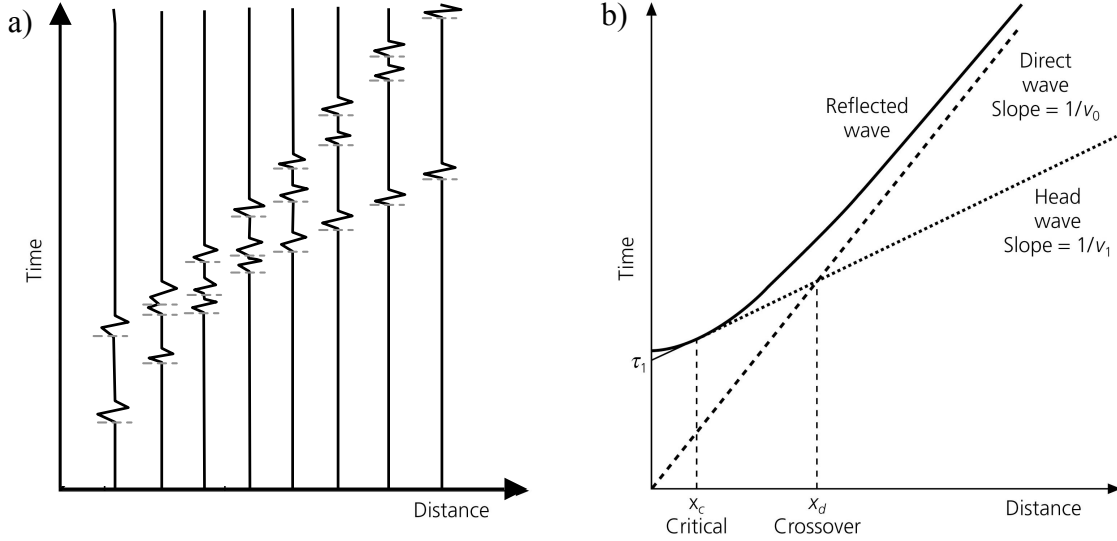


Fig 9. (a) Schematic section showing seismograms as a function of offset (distance), with time picks of various P-waves. (b) Travel time curves for rays in a layer over a half-space (modified from Stein and Wysession, 2003).

## 2.2- Multiple horizontal layer

In the case of multiple horizontal layers (Fig 10), the expressions for the travel time curves are as follows:

$$T_D(x) = \frac{x}{v_0} \quad (13)$$

$$T_{Rn}(x) = px + 2 \sum_{j=0}^{n-1} \eta_j h_j \quad (14)$$

$$T_{Hn}(x) = \frac{x}{v_n} + 2 \sum_{j=0}^{n-1} h_j \left( \frac{1}{v_j^2} - \frac{1}{v_n^2} \right)^{1/2} \quad (15)$$

$$= \frac{x}{v_n} + \tau_n$$

where  $T_{Rn}$  denotes reflections off the top of layer  $n$ , and  $T_{Hn}$  denotes head waves traveling in layer  $n$ .

To characterize a model consisting of several horizontal layers, follow these steps:

- 1) plot the seismograms as a function of offset;
- 2) pick the arrival times of the various phases and connect the picks to obtain travel time curves (Fig 10);
- 3) estimate  $v_0-v_n$  from the slopes of the travel time curves (Fig 10);
- 4) obtain  $\tau_1-\tau_n$  from the intercepts of the head waves' travel time curves and the time axis (Fig 10);
- 5) estimate the thickness of the layers iteratively (starting with layer 0) using the inferred values of  $v_0-v_n$  and  $\tau_1-\tau_n$  in eq. 15 for  $x=0$  km and  $T_{Hn}(x)=\tau_n$ :

$$h_{n-1} = \frac{\tau_n - 2 \sum_{j=0}^{n-2} h_j \left( \frac{1}{v_j^2} - \frac{1}{v_n^2} \right)^{1/2}}{2 \left( \frac{1}{v_{n-1}^2} - \frac{1}{v_n^2} \right)^{1/2}} \quad (16)$$

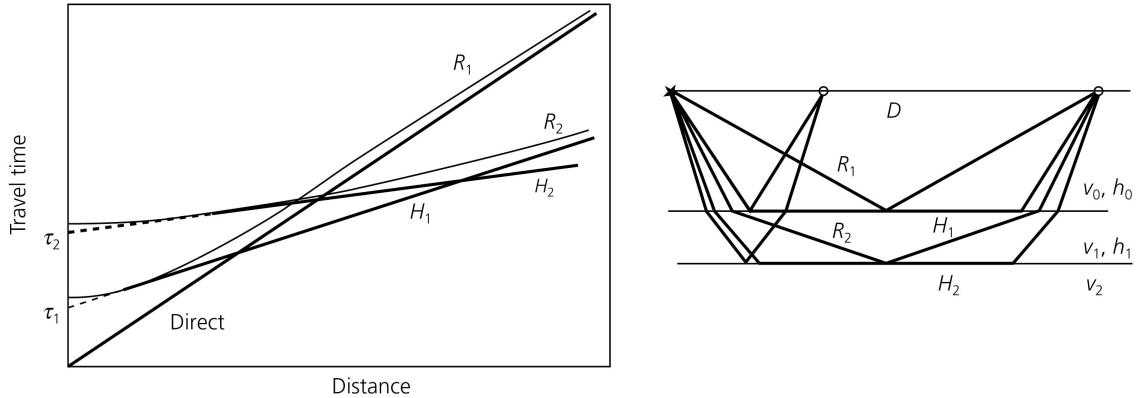


Fig 10. Travel times and rays for a model consisting of several horizontal layers (Stein and Wysession(2003)).

Note that this method is insensitive to low-velocity layers embedded in faster velocity material (Fig 11) and to thin layers (Fig 12). An example of a real seismic refraction record is shown in Fig 13.

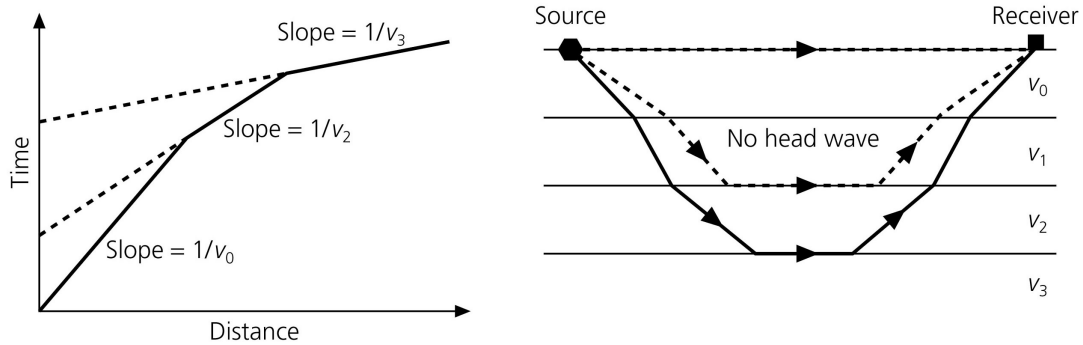


Fig 11. Travel times and rays for a model with a low-velocity zone (Stein and Wysession, 2003)

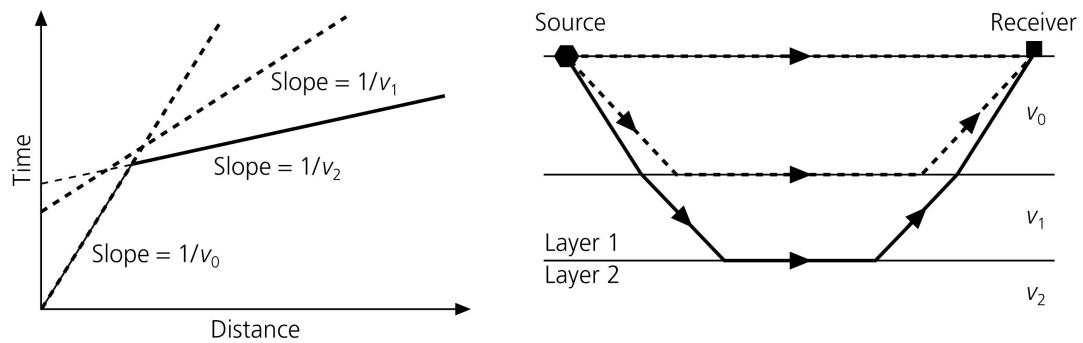


Fig 12. Travel times and rays for a model with a thin layer causing a blind zone (Stein and Wysession, 2003).

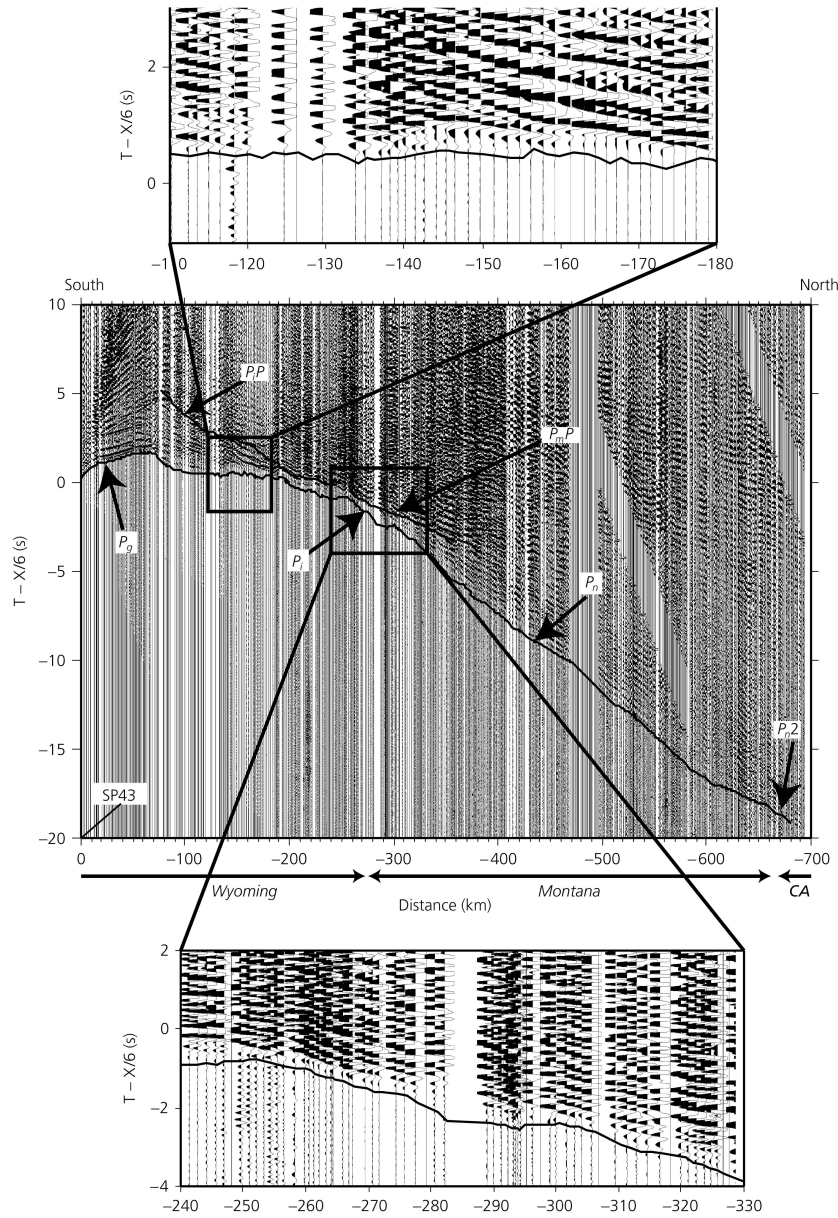


Fig 13. Example of a seismic refraction record section. Labels denote various P-waves traveling through the crust and mantle:  $P_g$ , direct P-wave;  $P_iP$ , wave reflected at crustal interface;  $P_i$ , head wave below crustal interface;  $P_mP$ , wave reflected at the Moho;  $P_n$ , head wave below the Moho;  $P_{n2}$ , head wave below mantle interface. Note the use of a reduced time scale on the time axis – this is done to facilitate the display of all the arrivals on a printout of manageable size (Stein and Wysession, 2003).

### 2.3- Dipping layer over a half-space

The refraction method can also be used to characterize simple 2-D models consisting of a dipping layer over a half-space – note that it is the interface between the upper layer and the half-space that is actually dipping in this case (Fig 13). Whereas the 1-D cases discussed in sections 2.1 and 2.2 required only one seismic source, the dipping layer

problem requires at least two seismic sources such that both a downdip and an updip rays can be recorded and analysed.

Travel times for the downdip and updip rays are described by the following expressions (Fig 14):

$$\begin{aligned}
 T_d(x) &= \frac{x \cos \theta - (2h_d + x \sin \theta) \tan i_c}{v_1} + \frac{(2h_d + x \sin \theta)}{v_0 \cos i_c} \\
 &= \frac{x \sin(i_c + \theta)}{v_0} + \frac{2h_d \cos i_c}{v_0}
 \end{aligned} \tag{17}$$

$$\begin{aligned}
 &= \frac{x}{v_d} + \tau_d \\
 T_u(x) &= \frac{x \cos \theta - (2h_u - x \sin \theta) \tan i_c}{v_1} + \frac{(2h_u - x \sin \theta)}{v_0 \cos i_c} \\
 &= \frac{x \sin(i_c - \theta)}{v_0} + \frac{2h_u \cos i_c}{v_0} \\
 &= \frac{x}{v_u} + \tau_u
 \end{aligned} \tag{18}$$

where  $T_d$  and  $T_u$  are the downdip and updip travel times,  $v_d$  and  $v_u$  are the apparent downdip and updip velocities, respectively, and all other parameters are defined on Fig 14. The dip angle and critical angle are expressed as follows:

$$\theta = \frac{1}{2} \left( \sin^{-1} \frac{v_0}{v_d} - \sin^{-1} \frac{v_0}{v_u} \right) \tag{19}$$

$$i_c = \frac{1}{2} \left( \sin^{-1} \frac{v_0}{v_d} + \sin^{-1} \frac{v_0}{v_u} \right) \tag{20}$$

To characterize this model (i.e., obtain estimates of  $v_0$ ,  $v_1$ ,  $h_d$ , and  $h_u$ ), find  $v_0$ ,  $v_d$ ,  $v_u$ ,  $\tau_d$ , and  $\tau_u$  from a record section displaying a reverse profile (Fig 13), and use these values in equations 17-20.

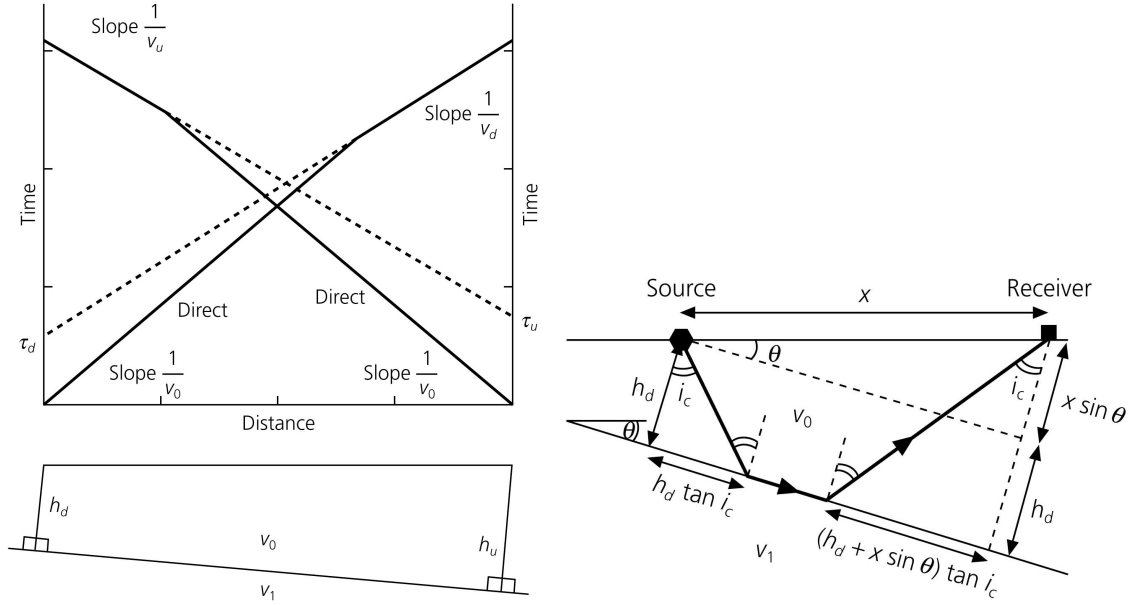


Fig 13. Travel times, model geometry and rays (downdip) for a dipping layer over a half-space (Stein and Wysession, 2003).

### 3- Seismic reflection

In applications to horizontally layered earth models, the seismic reflection technique is used to produce profiles outlining the vertical distribution and lateral extent of velocity/density discontinuities (interfaces) in the subsurface. It relies on the mapping of reflected P-waves as a function of horizontal distance along a profile. Source-receiver offsets are short compared to those used for refraction profiles ( $\sim 0-1$  times the depth of investigation). Instead of using one or two sources for a single profile, as in refraction, reflection sources are fired at every, or every second, receiver location to generate redundant data (Fig 14, 15).

In seismic reflection, redundant traces can be stacked into various forms of gathers to increase the signal-to-noise ratio of the reflected signal and emphasize certain features of the subsurface (Fig 14, 15). The signal-to-noise ratio increases by a factor of  $\sim \sqrt{N}$  for a stack of  $N$  traces. Here we will consider common midpoint (CMP) gathers, which are used to construct cross-sections of the subsurface. To properly stack seismic traces recorded at different source-receiver offsets, a time correction must be applied to each trace. This time correction is referred to as a Normal Moveout (NMO) correction, and it is calculated using the following equations (recalling eq. 14):

$$\begin{aligned} \Delta T_{NMO}(x) &= T_{Rn}(x) - t_n \\ &= px + 2 \sum_{j=0}^{n-1} \eta_j h_j - t_n \end{aligned} \quad (21)$$

where  $t_n$  is the two-way vertical travel time:

$$t_n = 2 \sum_{j=0}^n h_j / v_j \quad (22)$$

NMO curves for a layer over a half-space and for a multiple layer model are shown in Fig 16. If the velocities of the layers are not known, it is possible to search for the optimal velocities during stacking, i.e., different NMO velocities are used iteratively to search for the reflection pulse that exhibits maximum amplitude (Fig 17).

As in seismic refraction, it is possible to account for simple models consisting of a dipping layer over a half space. The geometry of the problem for this special case is shown in Fig 18, and the travel time of the reflected wave is given by the following expression:

$$T_R(x) = \frac{(x^2 + 4h^2 + 4hx \sin \theta)}{v_0^2} \quad (23)$$

A stacked CMP profile is shown in Fig 19. Note the imaging artifacts due to departures from the initial assumption that the model is horizontally layered. To get rid of these artifacts, seismologists migrate the data – migration is a processing technique that attempts to backproject scattered seismic energy recorded at the surface to its originating point at depth (see lower panel of Fig 19).

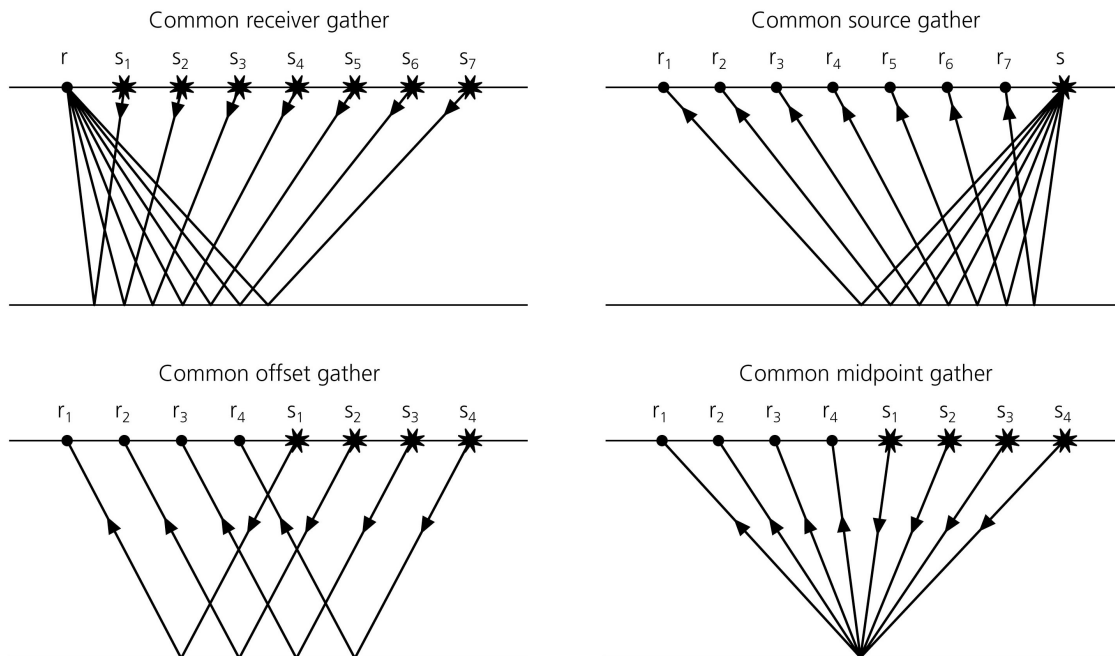


Fig 14. Various forms of trace gathers in seismic reflection (Stein and Wysession, 2003)

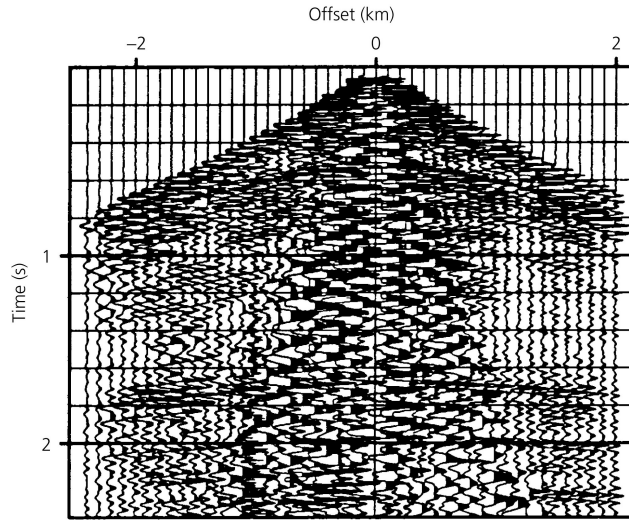


Fig 15. CMP gather (Stein and Wysession, 2003)

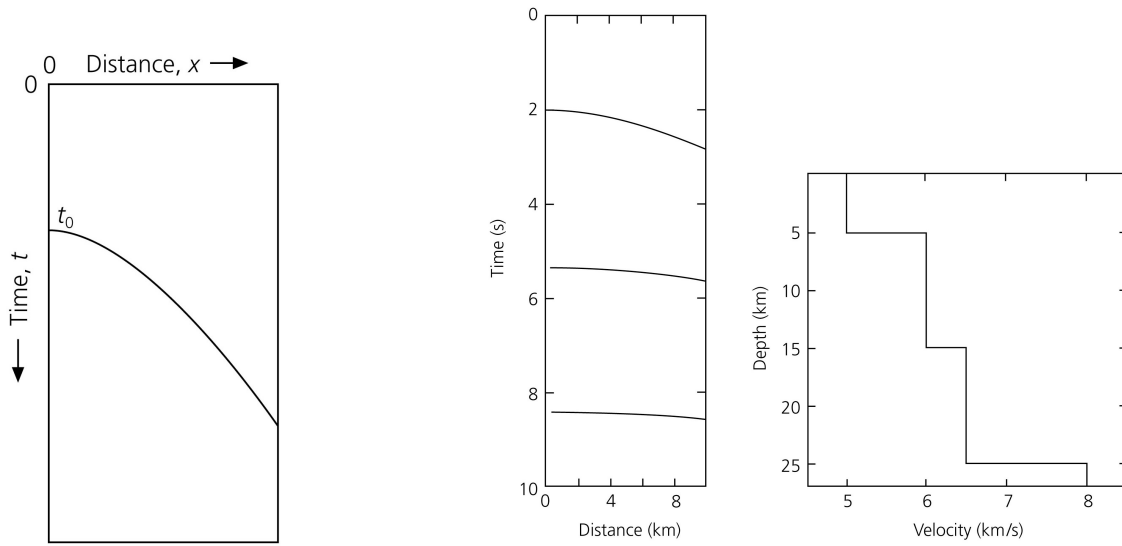


Fig 16. Left panel: travel time curve for reflected wave in a layer over a half space. Middle and right panels: travel time curve and velocity model for the case of waves reflected in a multiple layer model (Stein and Wysession, 2003).

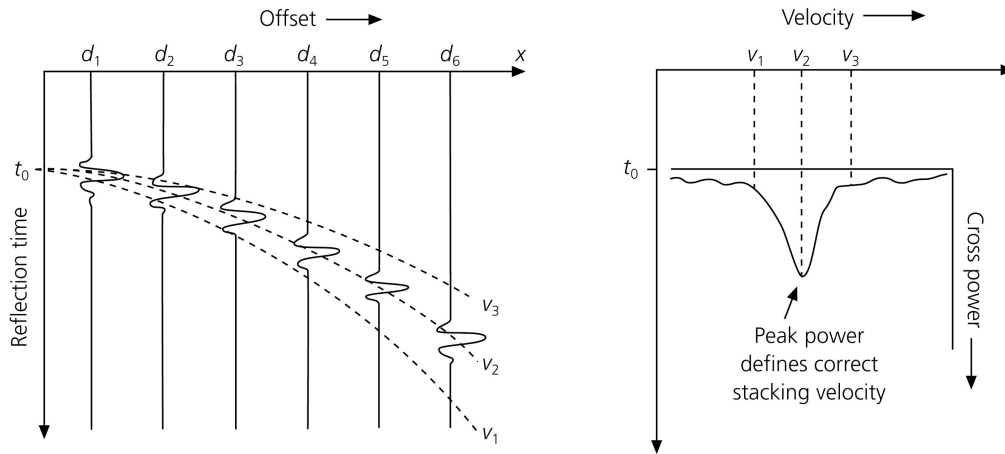


Fig 17. CMP stacks and velocity analysis. Left panel: schematic CMP gather, showing travel time (NMO) curves for various velocities. Right panel: CMP stacks along the dashed lines shown in left panel. The optimal stacking velocity is  $v_2$  (Stein and Wysession, 2003).

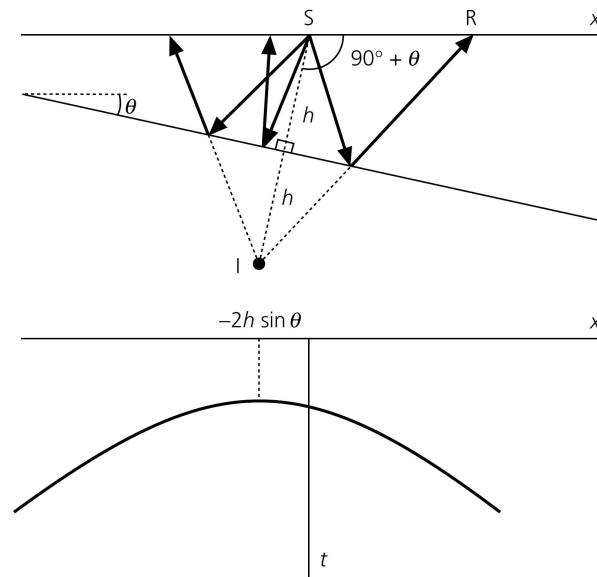


Fig 18. Rays and travel time curve for reflected waves in a dipping layer over a half space (Stein and Wysession).

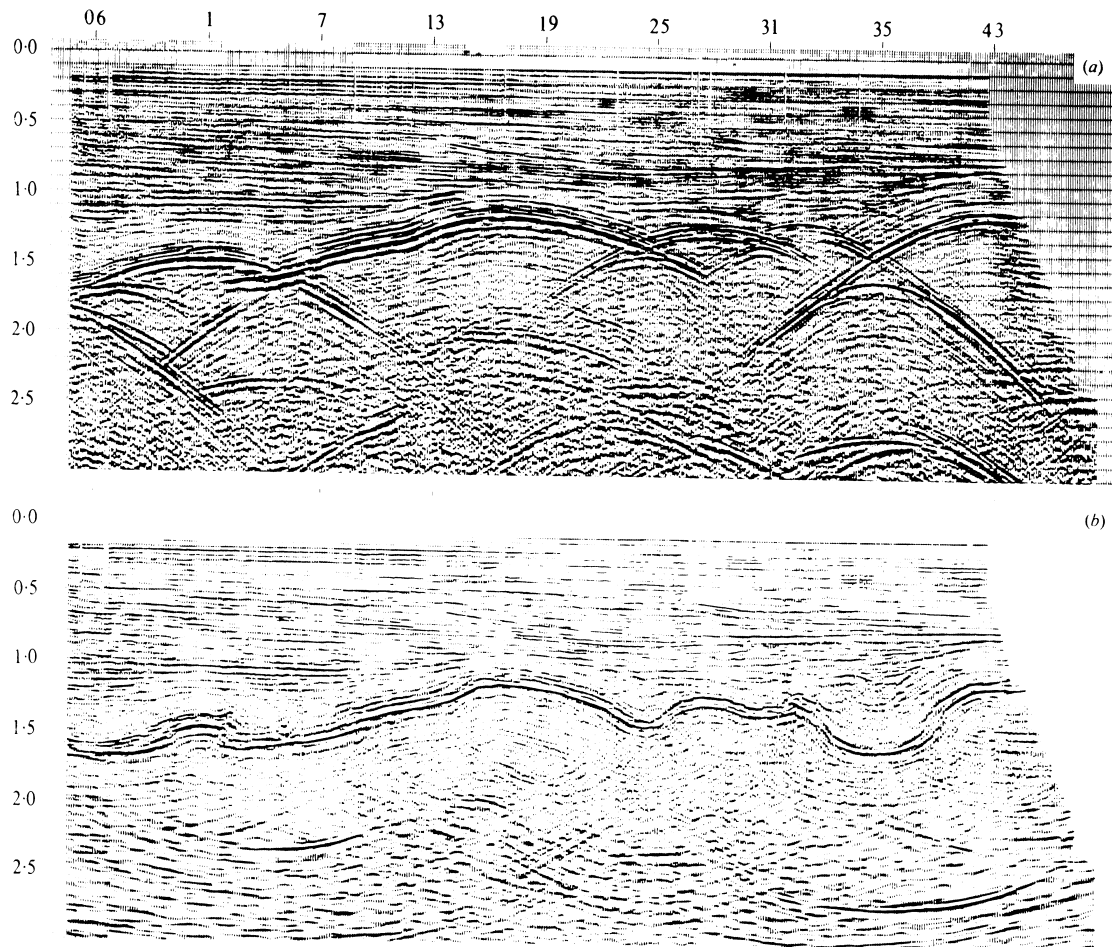


Fig 19. Seismic profile: CMP stacks (upper panel), migrated CMP stacks (lower panel). Taken from Sheriff and Geldart, 1995.

#### References

Sheriff, R.E. and R.P. Geldart (1995) *Exploration seismology*, Cambridge Univ. Press, Cambridge, 592 pp.

Stein, S. and M. Wysession (2003) *An introduction to seismology, earthquakes, and earth structure*, Blackwell Publishing, Oxford, 498pp.